

served above 50 °C in the molecular complex *cis*-[PtCl(PEt₃)₂-(Pd₂)] [BF₄].^{14e} The present result is quite remarkable: (i) It is evident that fluxionality of coordinated ligands transpires not only in molecular species but also in surface compounds. (ii) It illustrates a unique case in which a dynamic (fluxional) process is detected by a static (packing density) measurement; this is possible because the fluxional motion occurs at the expense of *close-packing* efficiency, and the decrease in efficiency is readily apparent from measurements of Γ .

Acknowledgment is made to the donors of the Petroleum Research fund, administered by the American Chemical Society, and to the Air Force Office of Scientific Research for support of this research.

Registry No. HQ, 123-31-9; BQ, 106-51-4; CAT, 120-80-9; 2,3-DMHQ, 608-43-5; 2,5-DMHQ, 615-90-7; DHQ, 527-18-4; TFHQ, 527-21-9; DHPy, 16867-04-2; DHPdz, 123-33-1; DHBM, 81753-11-9; THB, 4371-32-8; 2,6-AQDS, 84-50-4; DHT, 2889-61-4; NHQ, 571-60-8; Pt, 7440-06-4.

Contribution from the Department of Chemistry,
University of California, Santa Barbara, California 93106

Surface Coordination Chemistry of Platinum Studied by Thin-Layer Electrodes.¹ Surface Chemical Reactivity of Aromatic and Quinonoid Compounds Adsorbed in Specific Orientational States

MANUEL P. SORIAGA,* JAMES H. WHITE, DIAN SONG, VICTOR K. F. CHIA, PETER O. ARRHENIUS,
and ARTHUR T. HUBBARD*

Received March 12, 1984

The surface chemical reactivity of aromatic and quinonoid compounds chemisorbed at smooth polycrystalline Pt surfaces in specific coordination or orientational states has been investigated, primarily by thin-layer electrochemical and gas chromatographic techniques. Five reactions were studied as functions of mode of coordination, temperature, and surface (electrode) potential: (i) reversible electrochemical reactivity in adsorbed and free states; (ii) electrocatalytic oxidation of compounds exhibiting multiple orientational states; (iii) electrocatalytic hydrogenation of hydroquinone and S-attached thiophenol derivatives; (iv) exchange reactions between adsorbates; (v) substitution reactions between halides and aromatics. Reversible electroactivity in the adsorbed state was vastly different from that in the free state when the electroactive center was directly coordinated to the surface. The extent of catalytic oxidation or hydrogenation proved to be a sensitive function of initial orientation. Ring carbons close to the Pt surface underwent more drastic oxidation/hydrogenation than those further away. Hydrodesulfurization efficiency was influenced by the nature of the substituent directly linked to the -SH anchor. Ring hydrogenation that accompanied desulfurization was energetically favorable, but kinetically hindered. Ligand exchange/coadsorption reactions were functions of initial adsorbate orientation and concentration of species in solution. Appreciable exchange was noted only between molecules in η^2 -oriented layers and concentrated solutions. The influence of halides in ligand/coadsorption reactions decreased in the order $I^- \gg Br^- > Cl^- \gg F^-$. Simple aromatics were displayed virtually quantitatively by I^- . Alkyl substituents on the aromatic/quinonoid ring rendered it less labile, but its flat-adsorbed states underwent reorientation upon coadsorption of iodine.

Introduction

Studies described in the preceding article¹ have demonstrated spontaneous and irreversible adsorption of a variety of aromatic and quinonoid compounds at smooth polycrystalline Pt surfaces in specific orientational (coordination) states. The nature of these states has hitherto not been recognized because they emerge under conditions² neglected by previous investigations. For example, earlier studies of benzene adsorption at well-defined Pt single crystals in ultrahigh vacuum (UHV) employed sample pressures near 10^{-6} torr, at which only $\eta^6(\pi)$ -bonded intermediates are to be expected.³ The partial pressure corresponding to concentrations at which flat-to-vertical orientational transitions were observed for species adsorbed from aqueous solutions is about 20 torr.²¹ Prolonged and/or comparatively higher sample dosages were reported to induce reorientation of benzene adsorbed on Pt(111) and Pt(100).⁴

In the present article, surface chemical reactivities of selected diphenolic and quinonoid compounds² are described. Five reactions have been investigated with respect to mode of attachment, temperature, and electrode potential: (i) reversible electrochemical reactivity of the adsorbed state compared with that of the free state; (ii) electrocatalytic oxidation of compounds exhibiting multiple orientational states; (iii) electrocatalytic hydrogenation of hydroquinone and S-attached thiophenol derivatives; (iv) exchange reactions between nonidentical aromatic adsorbates; (v) substitution reactions between aromatics and halides. A few other studies of reactions of simple aromatics adsorbed on atomically flat or stepped Pt surfaces have been reported⁶ but only under conditions where mainly flat-adsorbed intermediates are present.²

Experimental Section

Experiments were based primarily on thin-layer voltammetry and coulometry.⁵ Thin-layer electrodes (TLE) employed in this work have been described, and their performance in surface chemical studies has been described.¹ The aqueous solutions contained molar perchloric or sulfuric acid supporting electrolyte. Product identification utilized gas chromatographic techniques.

Electrochemical Reactivity of Adsorbed Intermediates. The subject compounds display reversible two-electron quinone/diphenol reactivity

- (1) Soriaga, M. P.; Binamira-Soriaga, E.; Hubbard, A. T.; Benziger, J. B.; Pang, K.-W. P. *Inorg. Chem.*, preceding paper in this issue.
- (2) For parts a-q see ref 2 of the preceding paper in this issue.
- (3) Fischer, T. E.; Kelemen, S. R.; Bonzel, H. P. *Surf. Sci.* **1977**, *64*, 157. Richardson, N. V.; Palmer, N. R. *Surf. Sci.* **1982**, *114*, L1. Netzer, F. P.; Matthew, J. A. D. *Solid State Commun.* **1979**, *29*, 209. Lehwald, S.; Ibach, H.; Demuth, J. E. *Surf. Sci.* **1978**, *78*, 577. Gavezzotti, A.; Simonetta, M. *Surf. Sci.* **1982**, *116*, L207.
- (4) Gland, J. L.; Somorjai, G. A. *Adv. Colloid Interface Sci.* **1976**, *5*, 205. Stair, P. C.; Somorjai, G. A. *J. Chem. Phys.* **1977**, *67*, 4361.
- (5) Hubbard, A. T. *CRC Crit. Rev. Anal. Chem.* **1973**, *3*, 201.

- (6) (a) Tsai, M.-C.; Muetterties, E. L. *J. Am. Chem. Soc.* **1982**, *104*, 2534. (b) Tsai, M.-C.; Muetterties, E. L. *J. Phys. Chem.* **1982**, *86*, 5067. (c) Surman, M.; Bare, S. R.; Hofmann, P.; King, D. A. *Surf. Sci.* **1983**, *126*, 349.

in the unadsorbed state.^{2a} Similar electrochemical reactivity in the adsorbed form of known orientational state was investigated by cyclic voltammetry after removal of unadsorbed material by rinsing the thin-layer cavity with pure supporting electrolyte. The amount of electroactive surface-coordinated species (Γ_{el}) was quantitated by coulometry: $\Gamma_{el} = (Q - Q_b)_{el}/2FA$, where $(Q - Q_b)_{el}$ is the charge for reversible electrolysis of adsorbed material at potentials where the unadsorbed form reacts, F the Faraday constant, and A the metal surface area.

Electrocatalytic Oxidation. The effective stoichiometries of the oxidation reactions were characterized by n_{ox} , the average number of electrons for oxidation and complete desorption of the oriented-adsorbed intermediates. Changes in n_{ox} indicate changes in oxidation product distribution: chemisorbed molecule \rightarrow oxidation products + $n_{ox}e^-$. Values of n_{ox} were extracted from coverage (Γ)^{1,2n} and oxidation data by the use of Faraday's law: $n_{ox} = Q_{ox}/FAT$, where Q_{ox} is the charge for electrocatalytic oxidation of adsorbed material (in the absence of unadsorbed species, corrected for background oxidation of the Pt surface). Oxidation was carried out at a potential just below that for evolution of molecular oxygen, 1.18 V (Ag/AgCl reference) in 1 M perchloric acid.

Preliminary identification of products from oxidation of η^2 -hydroquinone (HQ) consisted of the following: (i) Pooled samples from the low-area, small-volume thin-layer electrodes were accumulated by spraying the contents of the TLE into a cooled centrifuge tube. After about 30 collections, the tubes were centrifuged to consolidate the liquid (ca. 120 μ L). A slight excess of KCl was added to the sample to precipitate $KClO_4$. After a second centrifugation, the liquid was lyophilized, and the organic products were extracted with redistilled pyridine; the resulting pyridine solution was silylated with bis(trimethylsilyl)trifluoroacetamide (BSTFA) containing 1% trimethylchlorosilane, by following published procedures.⁷ The reaction mixture was separated with a Perkin-Elmer Sigma 3B gas chromatograph equipped with a 3-m OV-17 column and a flame-ionization detector. Control experiments were also performed for reference samples of putative products and for a sample containing only supporting electrolyte. (ii) In a subsequent experiment, a comparatively large-area (168 cm²) and -volume (0.9 mL) thin-layer cell was constructed with Pt foil held in place between concentric precision glass tubes. The product mixture was analyzed for *maleic acid* as follows: the mixture was passed through a narrow glass column packed with an aqueous slurry of charcoal-Celite at a flow rate of 0.5 mL min⁻¹. The column was then washed with water and eluted with concentrated NH_4OH . The effluent was evaporated at 80 °C under a stream of nitrogen; BSTFA in dimethylformamide was added to the residue. The silylation reaction was carried out at 25 °C for 20 h. Chromatography was performed with a Hewlett-Packard 5840A gas chromatograph, equipped with a flame ionization detector and 15-m DB-1 capillary column.

Electrocatalytic Hydrogenation. Three thiophenol derivatives were studied: pentafluorothiophenol (PFT), 2,5-dihydroxythiophenol (DHT), and 2,5-dihydroxy-4-methylbenzyl mercaptan (DHBM). The reactions were carried out in 1 M $HClO_4$ at -0.200 V for 60 s. Quantitative scission of the C-S bond *without impairment of the aromatic/quinonoid moiety* (simple hydrodesulfurization) was indicated by a two-electron hydrogenation peak; otherwise, desulfurization was accompanied by ring hydrogenation/hydrogenolysis. The relative extents of these reactions were determined from the initial adsorbed amount ($\Gamma = \Gamma_{el}$), quantity of desulfurized-but-intact diphenol ($\Delta\Gamma_{des}$), and unreacted starting material ($\Gamma_{el,f}$): fraction desulfurized = $\Delta\Gamma_{des}/\Gamma$; fraction ring hydrogenation = $[\Gamma - (\Delta\Gamma_{des} + \Gamma_{el,f})]/\Delta\Gamma_{des}$ and $\Gamma_{el,f}$ for DHT and DHBM were measured by thin-layer coulometry.¹

Insight concerning hydrogenation of surface-coordinated HQ was obtained from n_{ox} vs. E_{ads} curves, where E_{ads} is the potential at which adsorption was carried out.²⁰ At potentials below -0.10 V, HQ adsorption was accompanied by H atom coadsorption, which led to partial hydrogenation. The extent of hydrogenation was reflected by the increase in n_{ox} at $E_{ads} < -0.10$ V relative to values at potentials where no surface H was present.

Ligand (Adsorbate) Exchange. Although ligand-exchange studies are usually based upon the use of isotopically labeled species, this study employed two compounds (HQ and 1,4-naphthohydroquinone (NHQ)) which, although nonidentical, display very similar adsorption characteristics.^{2b-d} These experiments focused on displacement and coadsorption reactions: exposure of surface η^{10} -NHQ to 0.1 mM HQ solution and,

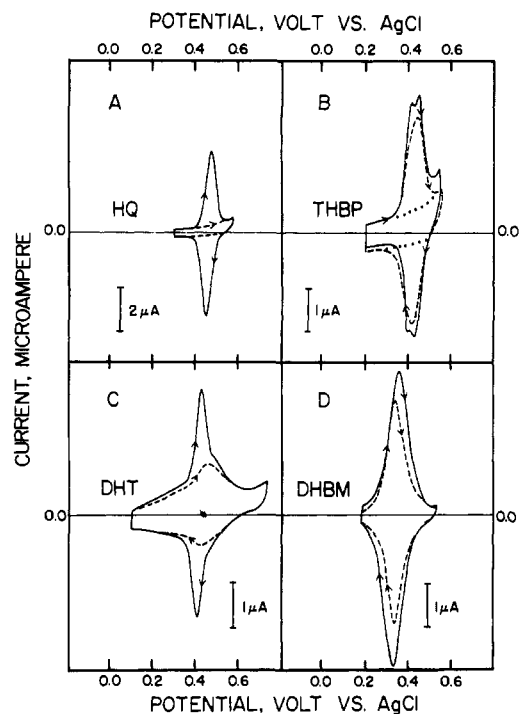


Figure 1. Thin-layer current/potential curves for the reversible quinone/diphenol reaction of (A) hydroquinone (HQ), (B) 2,2',5,5'-tetrahydroxybiphenyl (THBP), (C) 2,5-dihydroxythiophenol (PHT), and (D) 2,5-dihydroxy-4-methylbenzyl mercaptan (DHBM) at a polycrystalline Pt electrode: (—) in the presence of unadsorbed material ($C^0 = 0.1$ mM); (----) chemisorbed species only, η^2 -HQ, η^2 -THBP, $S-\eta^1$ -DHT, $S-\eta^1$ -PHBM; (---) adsorbed η^{12} -THBP. Thin-layer volume, $V = 4.08$ μ L; surface area, $A = 1.18$ cm²; rate of potential sweep, $r = 2.00$ mV s⁻¹; temperature, $T = 23 \pm 1$ °C; supporting electrolyte 1 M $HClO_4$.

likewise, η^{10} -NHQ to 2 mM HQ, η^2 -NHQ to 0.1 mM HQ, and η^2 -NHQ to 2 mM HQ and the opposite experiments exposing η^6 - or η^2 -HQ to 0.1 or 2 mM HQ. *Starting material* displaced from the preadsorbed layer or adsorbed from the solution was detected by thin-layer cyclic voltammetry and quantitated by thin-layer coulometry.¹

Ligand Substitution. Displacement and coadsorption reactions between halides (F^- , Cl^- , Br^- , I^-) and selected compounds were studied with regard to (i) concentration-dependent adsorption of organic adsorbates on halide-pretreated surfaces and (ii) displacement of adsorbed aromatics by halide. The former experiments measured the extent of displacement of coordinated halide while the latter probed the influences of mode of bonding of adsorbed organic species, halide concentration, and interfacial potential.

Results and Discussion

Reversible Electrochemical Reactivity. Figure 1 shows thin-layer current/potential curves for adsorbed and unadsorbed HQ, DHT, DHBM, and 2,2',5,5'-tetrahydroxybiphenyl (THBP) in the potential region where the unadsorbed form underwent reversible two-electron quinone/diphenol redox. The electroactivity of adsorbed HQ, regardless of orientation, was vastly different from that of the unadsorbed species. For THBP, reversible electron-transfer activity was displayed only for the orientation in which one HQ moiety was η^2 -coordinated and the other pendant; only one redox was present because the HQ group responsible for attachment to the surface was unreactive. PHT and DHBM are attached to the surface exclusively through the -SH substituent,¹ which resulted in reversible electroactivity of the pendant HQ moiety. The width of the voltammetric peak for $S-\eta^1$ -DHT was much greater than that for the unadsorbed material, apparently due to inductive effects operating through the metal; these were readily deactivated by introducing a -CH₂- link between the anchor and pendant electroactive center (as in DHBM).

Figure 2 shows total (Γ_T) adsorption profiles for THBP and phenylhydroquinone (PHQ) along with the respective isotherms for reversibly electroactive (Γ_{el}) coordinated material. For the

(7) Gates, S. C.; Dendramis, N.; Sweeley, C. C. *Clin. Chem. (Winston-Salem, N.C.)* 1978, 24, 1674. Thompson, J. A.; Markey, S. P. *Anal. Chem.* 1975, 47, 1313.

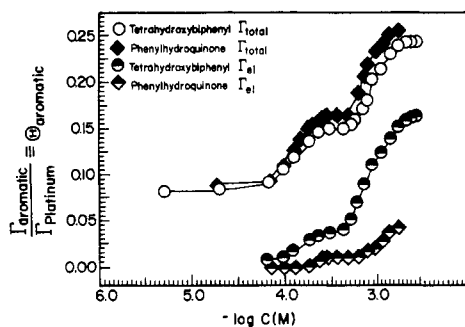


Figure 2. Adsorption isotherms for total and reversibly electroactive species of 2,2',5,5'-tetrahydroxybiphenyl and phenylhydroquinone. Θ is defined as $\Gamma/\Gamma_{\text{Pt}}$, where Γ_{Pt} is 2.35 nmol cm⁻² for a smooth polycrystalline Pt. Experimental conditions were as in Figure 1. The relative standard deviations in Γ were $\pm 3\%$ below 1 mM, $\pm 6\%$ above 1 mM. The solid lines interconnect experimental points and do not represent any theoretical curve.

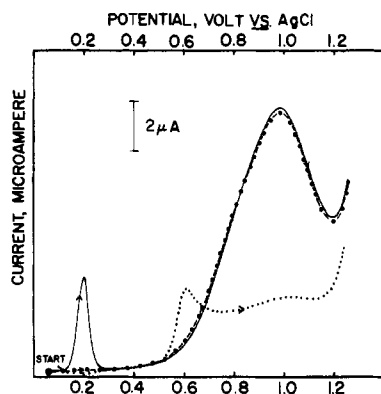


Figure 3. Thin-layer current/potential curve for electrocatalytic oxidation of 1,4-naphthoquinone at a smooth polycrystalline Pt surface: (—) in the presence of 0.1 mM dissolved material; (-·-) η^6 -coordinated material only; (···) clean surface. Experimental conditions were as in Figure 1.

η^2 -orientation, Γ_{el} for THBP was much greater than for PHQ, indicating preferential adsorption of the HQ moiety relative to the phenyl ring.¹ For THBP, the fraction $\Gamma_{\text{el}}/\Gamma_{\text{T}}$ increased with temperature,^{2j} implying that temperature-dependent factors other than orientation are important for this compound. For DHT and DHBM, $\Gamma_{\text{el}}/\Gamma_{\text{T}}$ was virtually independent of temperature, although the voltammetric peak width for DHT decreased at 65 °C.

Figures 1 and 2 illustrate a characteristic trait displayed by all of the subject compounds at Pt surfaces; electrochemical reactivity was sharply altered by *direct coordination of the electroactive center* to the metal surface. (The search for reversible redox potentials for adsorbed intermediates in aqueous solutions was hampered by irreversible hydrogenation (or oxidation) processes, even at moderately negative (or positive) potentials.¹) The severity of change in reactivity is a sensitive function of the strength of bonding to the surface; the shift in reversible redox potential is a measure of the relative binding strengths of reduced and oxidized species.¹ Changes in ligand electroactivity resulting from coordination to a metal center are not uncommon. For example, the reversible one-electron reduction of free duroquinone (DQ) in aprotic media is 500 mV more positive than in (1,5-cyclooctadiene)(duroquinone)nickel but 120 mV more negative than in bis(duroquinone)nickel.⁸

Electrocatalytic Oxidation. Thin-layer current/potential curves for irreversible oxidation of η^{10} -NHQ at 25 °C are shown in Figure 3. The solid curve was obtained in the presence of dissolved material (evidenced by the sharp peak at 0.20 V); the dot/dash

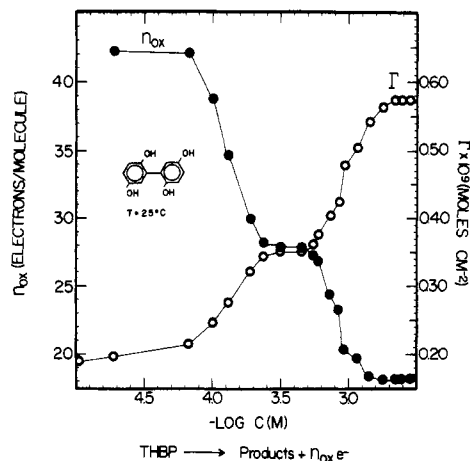
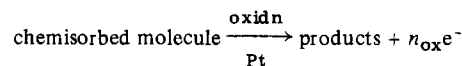


Figure 4. Adsorption (Γ) and oxidation (n_{ox}) isotherms for 2,2',5,5'-tetrahydroxybiphenyl. n_{ox} is a measure of the extent of oxidation of adsorbed material. Experimental conditions were as described in the text and in Figure 1. The relative standard deviations in n_{ox} and Γ were $\pm 3\%$ below 1 mM, $\pm 6\%$ above 1 mM. The solid lines interconnect data points and do not represent any theoretical curve.

Table I. Electrocatalytic Oxidation of Selected Aromatic Compounds Adsorbed on Platinum

compd	orientation	n_{ox}^a
hydroquinone	flat	22.4 \pm 0.6
	2,3- η^2	14.8 \pm 0.4
benzoquinone	flat	22.4 \pm 0.6
	2,3- η^2	14.6 \pm 0.4
methylhydroquinone	flat	28.3 \pm 0.9
	5,6- η^2	18.8 \pm 0.6
2,3-dimethylhydroquinone	flat	31.8 \pm 1.0
	5,6- η^2	17.1 \pm 0.5
2,5-dimethylhydroquinone	flat	33.0 \pm 1.0
	2,3- η^2	19.8 \pm 0.6
2,2',5,5'-tetrahydroxybiphenyl	flat	42.1 \pm 1.2
	2,3,5',6'- η^4	27.8 \pm 0.8
	3,4- η^2	18.1 \pm 0.6
1,4-dihydroxynaphthalene	flat	35.8 \pm 1.0
	2,3- η^2	18.0 \pm 0.8

^a n_{ox} is a measure of the reaction stoichiometry



Temperature, $T = 25$ °C.

curve is for adsorbed species only. The two curves were identical above 0.5, indicating that oxidation of *unadsorbed* naphthoquinone (NQ), the only species in solution above 0.20 V, was negligible. Clearly, the adsorbed intermediate underwent oxidation much more readily than the unadsorbed starting material. The stoichiometry of adsorbed molecule oxidations depends upon mode of attachment. This is illustrated in Figure 4, which shows the number of electrons (n_{ox}) transferred per molecule in the oxidation and complete desorption of THBP adsorbed in various orientational states (indicated by the packing density transitions). Oxidation stoichiometry, represented by n_{ox} , varies sharply with adsorbed molecule orientation. Data for other compounds are given in Table I. Invariably, the extent of catalytic oxidation was lower for vertical than for flat orientations.

The effect of temperature on n_{ox}^{2k} is illustrated by the data in Figure 5 for HQ and NHQ: (i) the correlation of n_{ox} with orientation persists at all temperatures (cf. Figure 6 of the preceding article); (ii) below 65 °C, $n_{\text{ox}}(\text{flat}) > n_{\text{ox}}(\text{edgewise})$. The magnitude of n_{ox} for any orientation approached an upper limit as the temperature was increased: 24 for HQ, 42 for NHQ. These values provide insight concerning the oxidation state of adsorbed intermediates. For example, 24 electrons is 2 less than expected for complete oxidation of unadsorbed HQ to CO₂; this is consistent

(8) Nesmeyanov, A. N.; Peganova, T. A.; Denisovich, L. I.; Isaeva, L. S.; Makarovskaya, A. G. *Dokl. Akad. Nauk SSSR* 1976, 230, 1114.

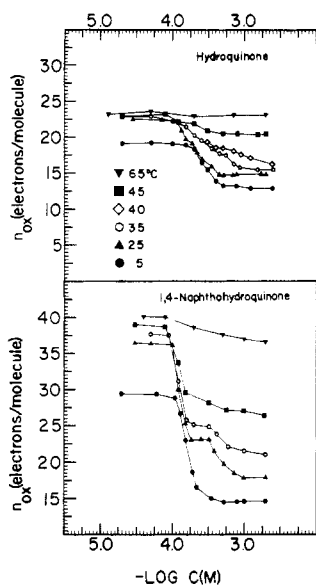


Figure 5. Oxidation (n_{ox}) isotherms for surface-coordinated hydroquinone and naphthohydroquinone at selected temperatures. Experimental conditions were as in Figure 4, except that, at 65 °C, the relative standard deviations in n_{ox} and Γ were twice as large as those at lower temperatures. The solid lines interconnect data points and do not assume any theoretical curve.

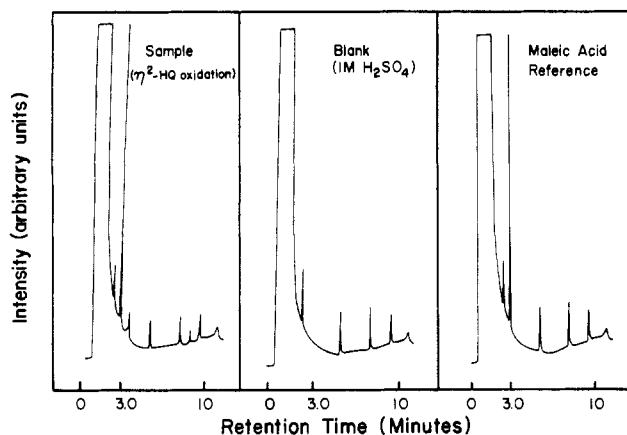


Figure 6. Gas chromatogram of a silylated product mixture obtained from electrocatalytic oxidation of η^2 -hydroquinone; the analytical procedure was specific for maleic acid. Experimental conditions were as described in the text.

with the observation that HQ undergoes a spontaneous 2-electron oxidation/dehydrogenation upon adsorption (to BQ in the η^6 -orientation and to a doubly dehydrogenated diphenolic species in the η^2 -orientation).¹ The virtual identity of $n_{ox}(\text{HQ})$ and $n_{ox}(\text{BQ})$, regardless of orientation, is evidence that the same surface-coordinated species is produced whether adsorption is from HQ or BQ solutions.¹

Examination of n_{ox} data at room temperature indicates that intermediates adsorbed in the flat orientation were not detached from the surface short of total conversion to CO_2 . Evidently, carbon atoms in intimate contact with the Pt surface underwent complete oxidation to CO_2 , and the extent of oxidation of the ring carbons in vertically oriented species varied with the proximity of each carbon to the metal surface. The measured value of n_{ox} for oxidation of 2,3- η^2 -HQ at 25 °C is consistent with conversion of the 2,3-carbons to CO_2 and milder oxidation of the remaining (four-carbon) fragment to maleic acid or tartaric acid.^{2h,i} Chromatographic analysis of the product mixture from η^2 -HQ oxidation indicated the presence of maleic acid (Figure 6).

The adsorption and oxidation of HQ at electrode potentials where appreciable chemisorbed oxygen (surface oxide) was present

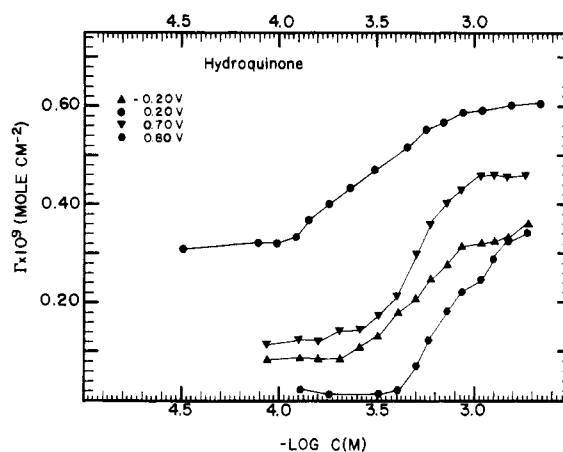


Figure 7. Adsorption isotherms for hydroquinone at selected electrode potentials. In these experiments, adsorption was done immediately at E_{ads} , in contrast to experiments in which adsorption was done initially at 0.200 V followed by potential change to E_{ads} (Figure 8).²⁰ All other experimental conditions were as in Figures 1 and 2.

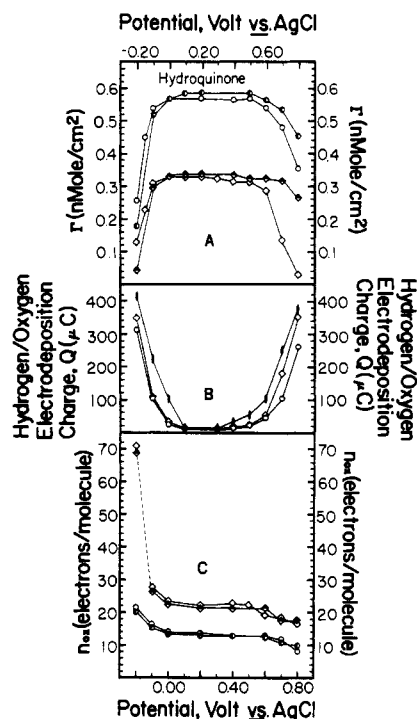


Figure 8. Effect of electrode potential on (A) packing density, (B) coadsorbed hydrogen/oxygen, and (C) oxidation reaction stoichiometry (n_{ox}) for hydroquinone adsorbed at 0.1 and 2 mM: (open diamonds) immediate adsorption at E_{ads} , $C^0 = 0.1$ mM; (half-filled diamonds) initial adsorption at 0.200 V and potential switched to E_{ads} , $C^0 = 0.1$ mM; (open circles) immediate adsorption at E_{ads} , $C^0 = 2$ mM; (half-filled circles) initial adsorption at 0.200 V and potential switched to E_{ads} , $C^0 = 2$ mM; (filled ovals) clean surface. The solid lines do not represent any theoretical curve. Experimental conditions were as in Figure 7.

has been studied.²⁰ The results, summarized in terms of adsorption profiles at various potentials (Figure 7) and Γ/n_{ox} vs. potential curves at selected concentrations (Figure 8), indicated that (i) adsorption of HQ at $E_{ads} > 0.6$ V in the presence of surface oxide was severely suppressed, (ii) despite this diminution of Γ , η^6 -oriented intermediates were still formed from dilute solutions and η^2 -adsorbed species from concentrated solutions, and (iii) allowing for partial oxidation of adsorbed organic species due to coadsorbed oxygen, the magnitude of n_{ox} for η^6 - or η^2 -coordinated intermediates was independent of whether adsorption occurred before or after surface oxide formation. Apparently, the product distribution from reactions in which the adsorbed intermediates were formed

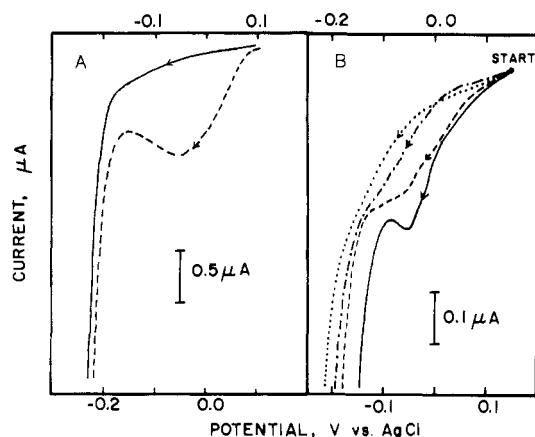


Figure 9. Initial negative-scan thin-layer voltammetric curves for (A) pentafluorothiophenol and (B) 2,5-dihydroxythiophenol. (A, 25 °C): (—) dissolved species with I-coated Pt electrode; (---) chemisorbed species only. (B, chemisorbed species only): (—) 65 °C; (---) 45 °C; (---) 5 °C. All other experimental conditions were as in Figure 1.

on the surface *prior* to oxidation (bare-metal electrocatalysis) was similar to that from processes in which adsorption occurs *after* surface oxidation (metal oxide electrocatalysis). Indeed, bulk electrolysis of a saturated solution of BQ in H_2SO_4 at PbO_2 electrodes yielded mainly maleic and tartaric acids;⁹ air oxidation of benzene or BQ over V_2O_5 yielded maleic acid.¹⁰ By analogy with homogeneous metal-catalyzed processes, metal oxide electrocatalysis may be likened to homolytic oxidation and bare-metal electrocatalysis to heterolytic oxidation.¹¹ The fact that oxidation of unadsorbed material was negligible at potentials where the adsorbed intermediates reacted readily (Figure 5) is an indication that oxidations catalyzed by native Pt metal proceed much faster than those catalyzed by Pt oxide. This rate difference arises because surface coordination is necessary for oxidation, but adsorption on surfaces covered with an oxide layer is suppressed (Figure 8). Bulk bare-metal catalysis requires reduction of the surface to regenerate active metal.

Electrocatalytic Hydrogenation. Figure 9A shows thin-layer current/potential scans over the hydrogen region at 25 °C for the adsorbed and unadsorbed forms of PFT; the latter result was obtained when the Pt electrode was precoated with iodine to prevent chemisorption of the PFT. The absence of a cathodic peak in the solid curve indicates that surface coordination was requisite for PFT hydrogenation at the potentials studied. The peak of the dashed curve is due to quantitative hydrodesulfurization.^{2j}

Figure 9B shows negative-scan voltammograms for chemisorbed DHT at selected temperatures. The absence of a well-defined peak at $T \leq 25$ °C indicates that hydrodesulfurization of DHT does not proceed as readily as that of PFT. This trend of increased stability towards desulfurization with decreased fluorination is attributable to the electronegativity of the F atoms; it is consistent with results from heterogeneous catalytic desulfurization studies which have shown that increased fluorination of thiophenol decreases its stability toward hydrogenolysis of the C-S bond.¹² The shift of the cathodic peak to less negative potentials with increase in temperature suggests that the desulfurization reaction involves appreciable activation energy.

Figure 10 gives thin-layer current/potential curves for DHT in the potential region of quinone/diphenol electroactivity, before and after electrochemical hydrogenation. The peaks obtained prior to desulfurization (solid curves) have been discussed above (cf.

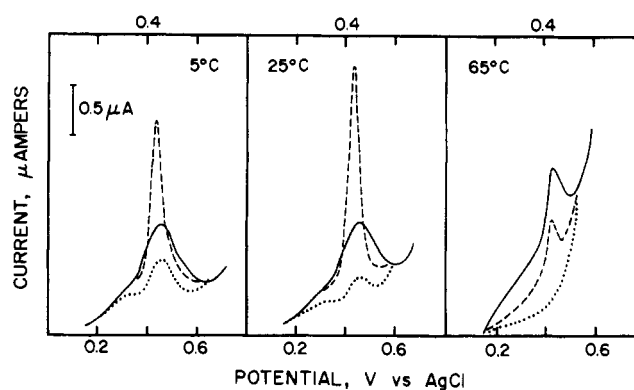
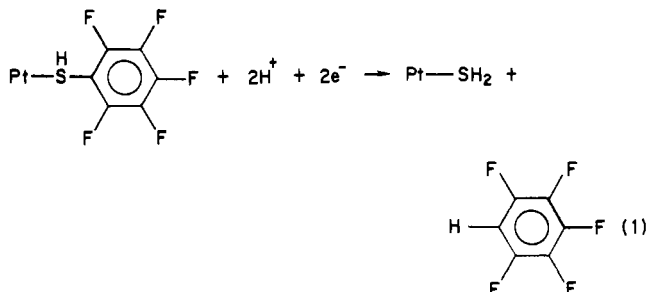


Figure 10. Thin-layer current/potential curves for the reversible diphenol to quinone oxidation of chemisorbed 2,5-dihydroxythiophenol: (—) before desulfurization; (---) after desulfurization, but without removal of desulfurized products; (---) after removal of desulfurized products. All other experimental conditions were as in Figure 1.

Table II. Electrocatalytic Hydrogenation of Chemisorbed Thiophenols at Selected Temperatures

compd	T , °C	% desulfurization (aromatic intact)	% ring hydrogenation
pentafluorothiophenol (PFT)	25	~100	~0
2,5-dihydroxythiophenol (DHT)	5	50	3.6
	25	71	21
	45	59	37
2,5-dihydroxy-4-methylbenzyl mercaptan (DHBM)	65	15	85
	5	5.0	~0
	25	15	~0

Figure 1c). The dashed curve corresponds to oxidation (to BQ) of the HQ produced from the reaction analogous to eq 1. The



peak was sharp because the HQ moiety was no longer bound to the -SH anchor. Γ is given by the area under the solid curve and $\Delta\Gamma_{\text{des}}$ by the area between the dashed and dotted curves. When the thin-layer cavity was rinsed with pure electrolyte after desulfurization, the detached HQ was rinsed away, and the subsequent voltammograms are given by the dotted curves, which define the amount of unreacted starting material $\Gamma_{\text{el.f}}$. The curves at 65 °C show that although hydrogenation was complete, the amount of desulfurized (but intact) HQ was greatly diminished; at this temperature, hydrogenation reactions that destroyed the aromatic functionality predominated.

Table II summarizes desulfurization/hydrogenation data: (i) The fact that the amount of desulfurized HQ decreased as the temperature was increased above 25 °C is an indication that ring-hydrogenation processes are energetically favorable but possess large activation barriers. (ii) Desulfurization efficiency is dependent on the nature of the functional group *directly attached* to the -SH moiety; the extent of desulfurization decreased in the order fluorinated phenyl (PFT) \gg phenyl (PHT) \gg alkyl (DHBM). (iii) Hydrogenation of the pendant diphenol was sharply diminished when the distance between the aromatic and the electrode surface was increased; this is in agreement with the observation that *unadsorbed* HQ was not hydrogenated under

(9) Kempf, R. J. *Prakt. Chem.* **1911**, *83*, 329.
 (10) Downs, C. R. *Ind. Eng. Chem.* **1940**, *32*, 1294.
 (11) Sheldon, R. A.; Kochi, J. K. *Adv. Catal.* **1976**, *25*, 274.
 (12) Reid, E. E. "Organic Chemistry of Bivalent Sulfur"; Chemical Publishing Co.: New York, 1958; Vol. VI, p 334.

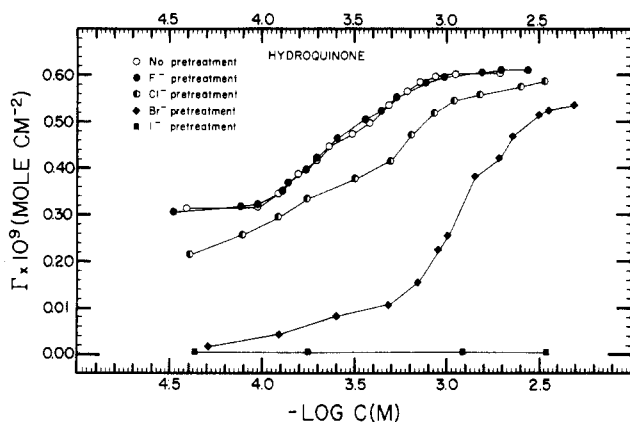


Figure 11. Adsorption of hydroquinone on halide-pretreated Pt surfaces, described in terms of Γ vs. $\log C^0$ curves. The solid lines simply interconnect the experimental points and do not assume any theoretical curve. Experimental conditions were as in Figures 1 and 2.

desulfurization conditions even at 65 °C.^{2j}

n_{ox} vs. E_{ads} curves for HQ are shown in Figure 8. HQ adsorption at -0.20 V resulted in partial hydrogenation, as evidenced by the fact that $n_{ox}(-0.20 \text{ V}) > n_{ox}(0.20 \text{ V})$. However, the difference between $n_{ox}(-0.20 \text{ V})$ and $n_{ox}(0.20 \text{ V})$ was much larger for intermediates adsorbed from low than from high concentrations and indicates that species initially adsorbed in the η^6 -orientation undergo much more drastic hydrogenation/hydrogenolysis than those coordinated in the η^2 -structure. Analogous to catalytic oxidation, the extent of hydrogenation of the ring carbons is apparently a function of their distance from the metal surface.

Ligand Substitution. The surface-coordination of HQ on Pt-halide surfaces, described in terms of Γ vs. $\log C$ curves, is illustrated by Figure 11. (i) The HQ adsorption isotherm was not influenced by F^- pretreatment. Evidently, displacement of adsorbed F^- by HQ occurred spontaneously. (ii) I^- pretreatment completely prevented HQ chemisorption; that is, HQ did not displace coordinated I^- . The inertness of iodine superlattices on Pt has been demonstrated under vacuum¹³ and in solution.^{14,15} (iii) The ease of halide displacement decreased in the order $F^- \gg Cl^- > Br^- \gg I^-$, a trend consistent with the relative strengths of halide coordination in molecular Pt complexes.¹⁶ (iv) Suppression of HQ adsorption by Cl^- and Br^- pretreatment was more dramatic at low than at high concentrations; above 3 mM, preadsorbed Cl^- and Br^- were eventually displaced, yielding an organic layer for which Γ was consistent with an η^2 -structure. These findings are quite surprising since the adsorption strength of η^6 -HQ was greater than that of η^2 -HQ, hence, adsorption in the flat orientation would expectedly be less affected by halide pretreatment. Apparently, other factors need to be considered.^{2p} For example, η^6 -coordination requires a greater number of contiguous sites initially occupied by sufficiently strongly adsorbed halide.

Figure 12 shows displacement of *starting material* when a surface pretreated with η^{10} - or η^2 -NHQ was exposed to dilute acidic iodide; as anticipated, the amount displaced ($\Delta\Gamma_{disp}$) was higher for η^2 - than for η^{10} -NHQ. Figure 12 is typical of simple diphenols.^{2b} $\Delta\Gamma_{disp}$ was also influenced by other factors, such as pH ($\Delta\Gamma_{disp}$ decreased as pH is increased) and adsorbate molecular structure (alkyl substituents lowered $\Delta\Gamma_{disp}$; DHT was not displaced by I^-).^{2b} Adsorbed reorientations from flat to vertical

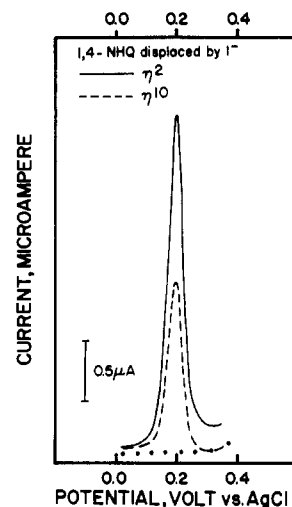


Figure 12. Thin-layer current/potential curve showing displacement of starting material when a Pt surface pretreated with η^{10} - or 2,3- η^2 -naphthohydroquinone was exposed to 0.5 mM I^- in 1 M $HClO_4$. Experimental conditions were as in Figure 1.

Table III. Displacement of Adsorbed 1,4-Naphthohydroquinone by Br^- and I^-

NHQ orientation	halide	concn, ^a M	potential, V vs. AgCl	$\Delta\Gamma_{disp}^{b,c}$ nmol cm ⁻²	$\Delta\Gamma_{disp}/\Gamma^c$
flat (η^{10})	Br^-	0.010	0.40	0.040	0.16
			0.20	0.040	0.16
			0.00	0.052	0.21
			-0.10	0.078	0.31
			-0.10	0.052	0.21
	I^-	0.001	0.20	0.052	0.21
			-0.10	0.094	0.38
			0.20	0.061	0.25
			-0.10	0.106	0.43
			-0.20	0.061	0.25
vertical (2,3- η^2)	Br^-	0.010	0.00	0.176	0.71
			-0.10	0.188	0.76
			0.00	0.212	0.86
			-0.10	0.228	0.92
			0.00	0.228	0.92
	I^-	0.001	0.40	0.092	0.16
			0.10	0.089	0.16
			0.00	0.118	0.21
			-0.10	0.141	0.25
			-0.20	0.106	0.19
I^-	0.010	0.20	0.113	0.20	
		0.00	0.148	0.26	
		-0.10	0.173	0.31	
		0.20	0.136	0.24	
		0.00	0.179	0.32	

^a The solutions contained 1 M $HClO_4$. ^b Reaction time was 3 min. ^c Initial Γ values for flat and vertical orientations were 0.247 and 0.564 nmol cm⁻², respectively. The average relative standard deviations in Γ and $\Delta\Gamma_{des}$ are $\pm 3\%$ below 1 mM, $\pm 6\%$ above 1 mM.

structures induced by coadsorption of iodine have been observed in solution^{2b} and under vacuum.¹⁷

Numerical results for displacement of surface-coordinated NHQ by Br^- and I^- are summarized in Table III:^{2a} (i) Virtually all of the initially adsorbed NHQ was displaced by 10 mM I^- at -0.10 V, regardless of orientation. Clearly, surface coordination of η^{10} - or η^2 -NHQ occurred without decomposition. (ii) The amount displaced by Br^- was considerably lower than that desorbed by I^- . Taken with the data in Figure 11, this result indicates that

- (13) Felner, T. E.; Hubbard, A. T. *J. Electroanal. Chem.* **1979**, *100*, 473. Garwood, G. A.; Hubbard, A. T. *Surf. Sci.* **1980**, *92*, 617.
 (14) Hubbard, A. T.; Stickney, J. L.; Rosasco, S. D.; Soriaga, M. P.; Song, D. *J. Electroanal. Chem. Interfacial Electrochem.* **1983**, *150*, 165. Stickney, J. L.; Rosasco, S. D.; Song, D.; Soriaga, M. P.; Hubbard, A. T. *Surf. Sci.* **1983**, *130*, 326.
 (15) Lane, R. F.; Hubbard, A. T. *J. Phys. Chem.* **1975**, *79*, 808.
 (16) Hartley, F. R. "The Chemistry of Platinum and Palladium"; Applied Science Publishers: London, 1973.

- (17) Katekaru, J. Y.; Garwood, G. A.; Hershberger, J. F.; Hubbard, A. T. *Surf. Sci.* **1982**, *121*, 396.

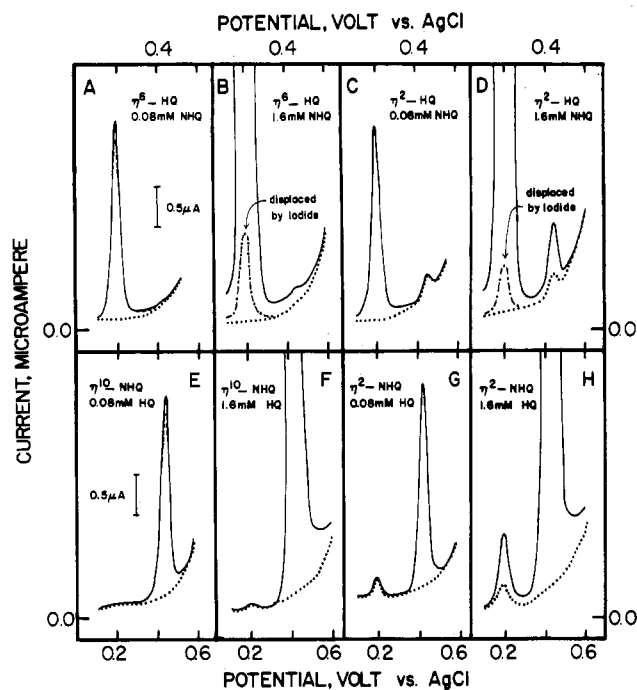
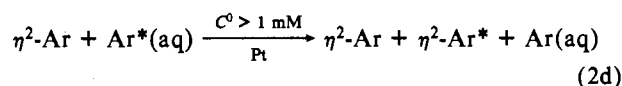
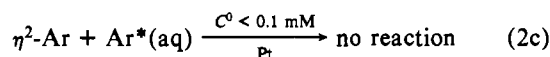
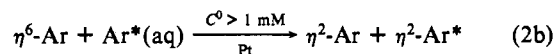
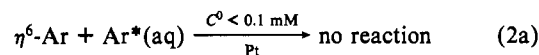


Figure 13. Thin-layer current-potential curves before (---) and after (—) exposure of a Pt surface pretreated with an oriented layer of 1,4-naphthoquinone (NHQ) or hydroquinone (HQ) to a single aliquot of 0.08 or 1.6 mM HQ (or NHQ). The peak at 0.20 V is due to unadsorbed NHQ and that at 0.46 V to unadsorbed HQ. The dot-dash curve is for NHQ displaced by iodide after the exchange/coadsorption reactions. Experimental conditions were as in Figure 1.

the (full coverage) adsorption strength of aromatic/quinonoid compounds is greater than that of HBr^{18} but lower than that of HI^{11} ; that is, $-30 \text{ kcal/mol} < \Delta G_{\text{ads}}^{\circ} < -20 \text{ kcal/mol}$, consistent with estimates based upon adsorption isotherms.¹ (iii) The extent of displacement ($\Delta\Gamma_{\text{disp}}/\Gamma$) appeared to be independent of initial orientation. (iv) The amount of desorbed NHQ increased slightly as the potential was decreased. Maximum desorption occurred at -0.10 V . Below -0.10 V , ligand substitution was complicated by hydrogenation side reactions, which destroyed the quinone/diphenol functionality prior to desorption. Evidently, increasingly negative surface charge weakened the organic species-Pt bond: (a) If surface coordination is a combination of ligand-to-metal electron donation (σ -bonding) and metal-to-ligand back-donation (π -back-bonding),¹⁶ one would expect that a large negative charge density on the metal surface would work against aromatic adsorption. (b) Given that π -BQ is favored in η^6 -attachment and di- σ -HQ in η^2 -coordination,¹ a large negative surface charge may lead to partial reduction or hydrogenation to form species that are less strongly bound.

Ligand Exchange. Figure 13A-D shows thin-layer current/potential curves obtained before (dotted curve) and after (solid

curve) exposure of a Pt surface pretreated with an oriented layer of HQ to a single aliquot of NHQ solutions of various concentrations. The peak at 0.20 V was due to oxidation of unadsorbed NHQ to NQ, while that at 0.46 V was due to oxidation of desorbed HQ to BQ. The amount of NHQ adsorbed onto the HQ-pretreated surface, measured identically with that on clean surfaces,¹ was verified by displacement with iodide (dot/dash curve). (i) No displacement of preadsorbed η^6 - or η^2 -HQ was effected by 0.08 mM NHQ. (ii) Adsorption of NHQ occurred from 1.6 mM solution onto η^6 -HQ-pretreated Pt, but displacement of HQ was not observed. Coadsorption of HQ and NHQ to this degree ($\Gamma_{\text{HQ}} = 0.3 \text{ nmol cm}^{-2}$; $\Gamma_{\text{NHQ}} = 0.2 \text{ nmol cm}^{-2}$) is possible only when both species are oriented vertically. (iii) Displacement of η^2 -HQ was induced by 1.6 mM NHQ, and the amount of HQ displaced ($0.09 \text{ nmol cm}^{-2}$) was the same as the amount of NHQ adsorbed. Results from the opposite experiments in which Pt pretreated with an oriented layer of NHQ was exposed separately to 0.08 and 1.6 mM HQ, shown in Figure 13E-H, were similar. The orientation and concentration dependence of adsorbate exchange reactions may be summarized as follows:



For Ar = HQ (or NHQ) and Ar* = NHQ (or HQ) at 25 °C and 180 s reaction time, only about 10% exchange (eq 2d) was noted when the potential was at -0.10 V . Under UHV conditions, $\eta^6\text{-C}_6\text{H}_6$ has been reported to exchange readily with C_6D_6 on Pt(111),^{6a} but not on Pt(100).^{6b} Although the latter result is in agreement with eq 2a, it is important to realize that while benzene was used in the UHV studies,⁶ diphenols were employed in the present study; adsorption of the subject diphenols in the flat orientation apparently yields π -bonded quinones,¹ and it is known that quinonoid compounds are much more strongly π coordinated to zerovalent Pt than benzene.¹⁹

Acknowledgment is made to the donors of the Petroleum Research Fund, administered by the American Chemical Society, and to the Air Force Office of Scientific Research for support of this research.

Registry No. HQ, 123-31-9; BQ, 106-51-4; THBP, 4371-32-8; PFT, 771-62-0; DHT, 2889-61-4; DIBM, 81753-11-9; NHQ, 571-60-8; PHQ, 1079-21-6; Br⁻, 24959-67-9; I⁻, 20461-54-5; Pt, 7440-06-4; H₂, 1333-74-0; O₂, 7782-44-7; methylhydroquinone, 95-71-6; 2,3-dimethylhydroquinone, 608-43-5; 2,5-dimethylhydroquinone, 615-90-7; 1,4-dihydroxynaphthalene, 571-60-8.

(18) Garwood, G. A.; Hubbard, A. T. *Surf. Sci.* **1982**, *12*, 281.

(19) Cennini, S.; Ugo, R.; La Monica, G. *J. Chem. Soc. A* **1971**, 416.